

Fluorine-19 solid-state NMR investigation of regiodefective semicrystalline α -poly(vinylidene fluoride)

Philip Wormald^a, David C. Apperley^{a,*}, Francois Beaume^b, Robin K. Harris^a

^a*EPSRC Solid-State NMR Service, Industrial Research Laboratories, University of Durham, South Road, Durham DH1 3LE, UK*

^b*Atofina, Centre d' Étude de Recherche et Développement, 27470 Serquigny, France*

Received 23 May 2002; received in revised form 31 October 2002; accepted 4 November 2002

Abstract

Solid-state ^{19}F NMR has been applied to poly(vinylidene fluoride) to investigate, inter alia, the location of the reverse units. The application of relaxation filters in pulse sequences revealed fundamental differences relating to the domain structure of PVDF. A $T_{1\rho}(\text{F})$ spin-lock experiment gave a spectrum of the crystalline phase along with some intensity from signals associated with reverse units. The proximity of reverse units to the amorphous and crystalline domains was further investigated by $T_{1\rho}(\text{F})$ -filtered radio frequency driven recoupling (RFDR) and spin-diffusion experiments. The results showed the majority of reverse units to be relatively mobile (i.e. amorphous). However, weak RFDR cross-peaks were detected which suggest the presence of some reverse units in relatively rigid domains. A signal arising from a highly mobile site was detected at $\delta_{\text{F}} = -115$ ppm by a delayed acquisition experiment and is tentatively assigned to $-\text{CH}_2\text{CF}_2\text{H}$ end-groups.

© 2002 Elsevier Science Ltd. All rights reserved.

Keywords: Poly(vinylidene fluoride); Nuclear magnetic resonance; Radio frequency driven recoupling

1. Introduction

The fluorine atom has a van der Waals radius of 0.135 nm, which is only slightly larger than that of hydrogen (0.12 nm) and forms highly polar bonds. A combination of this polarity and higher levels of structure in poly(vinylidene fluoride) (PVDF) influences the piezo- and pyro-electric properties of this polymer [1].

Poly(vinylidene fluoride) crystallises into four polymorphs, α , β , γ and δ , depending upon the thermal treatment administered [1]. The unit cell of the lattice of α -PVDF consists of two chains in the tg_+tg_- conformation. The dipole components are mutually antiparallel and therefore neutralise each other; hence it exhibits non-polar behaviour. A polar analogue to α -PVDF is δ -PVDF, which has a $tttg_+tttg_-$ conformation and is formed by the application of a high electric field [1]. This involves the rotation of every second chain by 180° about the chain axis whereby their dipole moments point in the same direction.

The most highly polar phase is the β phase. Its unit cell consists of two all-trans chains packed with their dipole moments pointing in the same direction.

Studies by X-ray diffraction and solid-state nuclear magnetic resonance (NMR) spectroscopy [2,3] have shown that when thermally treated and drawn, a blend of the α and β phases is inevitable. Transitions between polymorphs have been studied by a combination of differential scanning calorimetry (DSC), infrared spectroscopy and X-ray diffraction techniques [4,5]. These experiments showed that the α to β transition was most efficient between 70 and 90°C during drawing. The majority of researchers have concentrated their attention on the β polymorph because of its piezo- and pyro-electrical properties, giving subsequent industrial usage. However, these properties are affected by the presence of regiodefective, so-called reverse, units (see below). Lovinger et al. [6] showed that the sample temperature and the mole percentage of the reverse units were fundamental to the α/β ratio and thereby the physical properties of the material.

Solid-state magic-angle spinning (MAS) NMR has been shown to be an important technique for the characterisation of polymer morphology [7]. The high gyromagnetic ratio

* Corresponding author. Tel.: +44-191-374-2585; fax: +44-191-374-2591.

E-mail address: d.c.apperley@durham.ac.uk (D.C. Apperley).

and natural abundance of the ^{19}F nucleus gives high sensitivity and it has a wide chemical shift range. Solid-state ^{19}F NMR is therefore a powerful tool for the study of fluorine-containing polymers as discussed in two review articles by Harris and coworkers [8,9].

Holstein et al. [10] used solid-state ^{19}F NMR together with high-power ^1H decoupling to give increased chemical shift resolution for PVDF. Differences in relaxation behaviour of the crystalline and amorphous phases were used to edit the spectrum, thus revealing important details about the morphology of the material. In a later work from the same group [11] these differences in relaxation behaviour were utilised for domain selection in spin-diffusion experiments. The measurement of domain sizes and their dependence on the contact time during cross-polarisation MAS experiments incorporating relaxation filters was compared and found to be in agreement with static domain-size measurements [11]. Ando et al. [12] have also used solid-state NMR to study PVDF, putting emphasis on understanding the cross-polarization behaviour between two abundant spin systems.

Scheler [13] proved that MAS at 35 kHz effectively suppressed heteronuclear (H,F) dipolar interactions without the need for proton decoupling. He also used radio frequency driven recoupling (RFDR) [14] with high-speed MAS and showed that the reverse units had a spin exchange with the amorphous region. No exchange between the crystalline signal and resonances for the reverse units were detected, nor between signals for the two reverse units, suggesting that these bands originate from different types of fluorines which are separated in space. Su and Tzou [15] also applied fast MAS ^{19}F NMR to PVDF.

In this paper we compare the effects of direct polarisation with relaxation filters and debate the results in terms of domain selectivity with regard to the reverse units. A direct-polarisation delayed-acquisition (DPDA) experiment was applied to sample the long-time behaviour of the fluorine spin system [16]. A relaxation-selective Goldman–Shen spin-diffusion experiment [17] was employed to establish diffusion rates and domain sizes. An RFDR experiment [14] with spin-lock filter was employed to further understand the morphology of high molecular weight PVDF and the location of the reverse units.

2. Experimental

All solid-state spectra were recorded by direct ^{19}F polarisation, with ^1H decoupling, using a Varian UNITYplus spectrometer, operating at 299.95 MHz for ^1H and 282.21 MHz for ^{19}F , with a Doty XC5 $^1\text{H}/^{19}\text{F}$ probe. The spectral reference was a replacement sample of C_6F_6 ($\delta_{\text{F}} = -166.4$ ppm with respect to the usual standard CFCI_3) and ^1H decoupling was used during referencing so that corrections for the Bloch–Siegert shift [18] are not required. All spectra were recorded with a spin rate of

14 kHz. The probe temperature was calibrated by the methanol method [19]. Spinning at 14 kHz with a bearing gas supply at 20 °C corresponds to a sample temperature of ca. 60 °C. Silicon nitride rotors were used on all samples, with Vespel drive caps to avoid unwanted fluorine background signal. The sample volume was restricted to 70 μl to increase r.f. homogeneity. Experimental parameters were a 3.6 μs $\pi/2$ pulse duration for ^{19}F with a proton decoupling field during acquisition equivalent to 85 kHz and a 2 s recycle delay. Discrimination of the crystalline domains was achieved with a pre-acquisition fluorine spin-lock time of 25 ms at a RF field equivalent to 80 kHz. The pulse sequences used are shown in Fig. 1.

The solution-state spectra were recorded at 22 °C on a Varian Inova spectrometer, operating at 499.78 MHz for ^1H and 470.21 MHz for ^{19}F . The solvent was dimethylsulfoxide- d_6 ($\text{DMSO}-d_6$) and chemical shifts are quoted relative to the signal for a replacement sample of CFCI_3 .

A Perkin–Elmer Pyris 1 DSC with external nitrogen cryofill and a working temperature range from -180 to 260 °C was used for thermal analysis, including measurement of the crystallinity. Pyris Thermal Analysis software for Windows version 3.52 was used for instrument control and data analysis.

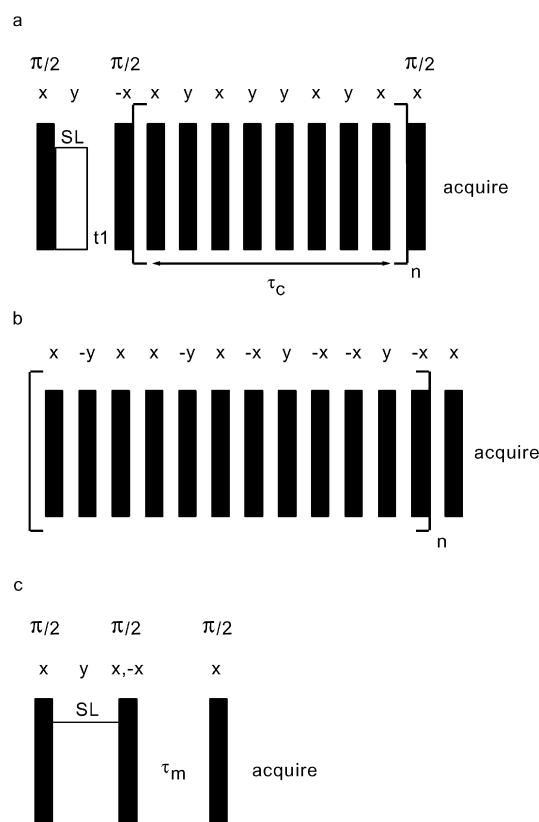


Fig. 1. Pulse sequences (with pulse phases) used in the present studies. All were implemented with CW proton decoupling during acquisition: (a) RFDR with a $T_{1\rho}(\text{F})$ relaxation filter, τ_c = RFDR mixing, looped n times, t_1 = evolution time; (b) dipolar filter looped n times ($n = 16$), and (c) the Goldman–Shen spin-diffusion experiment with a $T_{1\rho}(\text{F})$ relaxation filter, τ_m = mixing time. SL = spin-locking.

The nascent powder sample was Kynar 301F, supplied by Atofina France, with a molecular mass of 1×10^6 Da by GPC. A melting point of 158 °C and a crystallinity of 28% were obtained by DSC [20,21]. A reverse-unit content of 4.7% was determined by solid-state NMR. It should be noted that this sample has different characteristics from the ones discussed in our earlier publications [10,11].

3. Results

3.1. Solution-state NMR

The ^{19}F - $\{^1\text{H}\}$ spectrum of our sample of PVDF in solution in DMSO at 22 °C is shown in Fig. 2(a). The most intense peak arises from ^{19}F in CF_2 groups of regular $(\text{CF}_2\text{CH}_2)_n$ chains remote from any defects. Fig. 2(b) shows part of a polymer chain around a reversed unit, together with the lettering to distinguish the various fluorine sites. The spectrum is similar to those illustrated in the literature [22–31], though chemical shifts are sensitive to the nature of the solvent and the concentration. The assignments are indicated both on Fig. 2(a) and, together with the chemical shifts, in Table 1. They are in general agreement with those given in the literature (see especially Ref. [22]) and with our two-dimensional COSY experiments (see below). Apart from the labelled peaks, there are a number of weak signals

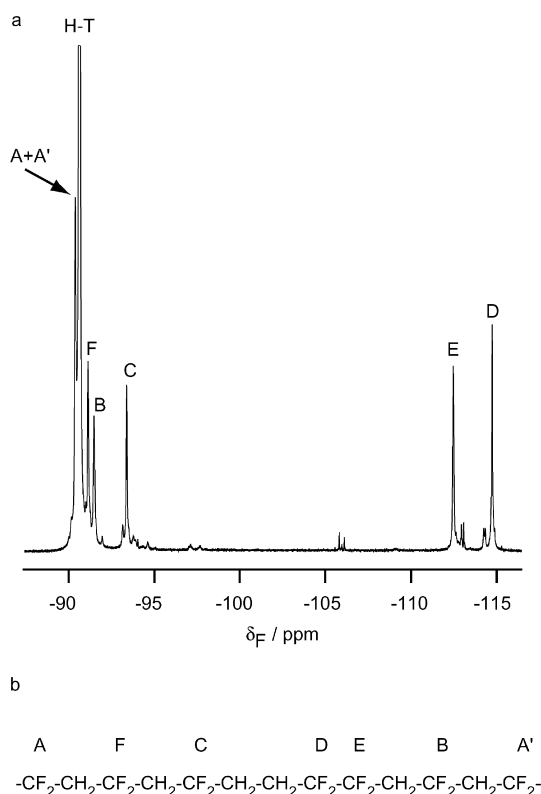


Fig. 2. (a) ^{19}F solution-state spectrum of PVDF in DMSO- d_6 at 22 °C. The labelling of the reverse unit is that shown in Fig. 2(b) and corresponds to the shifts in Table 1.

Table 1

Chemical shifts and assignments for the ^{19}F spectra of PVDF in solution in DMSO- d_6 at 22 °C and in the solid-state at ca. 60 °C

δ_F (ppm, solution)	Assignment	δ_F (ppm, solid)	Assignment
-90.92	A and A'	-82.1	Crystalline domains
-91.25	Main chain CF_2	-91.2	Amorphous domains
-91.71	F	-95.6	Crystalline domains
-92.07	B	~ -107	Chain branching ?
-93.97	C	-113.8	Reverse unit
-113.08	E	-114.9	Reverse unit
-115.35	D	~ -115	$-\text{CH}_2\text{CF}_2\text{H}$ end-groups ?

arising from the mode of synthesis. In general, these are not expected to be visible in spectra of solid PVDF. For instance, there is a group of small signals at $\delta_F = -106$ to -107 ppm (Fig. 2(a)), which has been attributed to end-groups, branches or oligomeric species, etc. [22,25,27,30,31]. However, in this case we have observed a small signal in our solid-state spectra. Fig. 3 shows the ^1H -coupled ^{19}F COSY spectrum of PVDF in DMSO- d_6 at 22 °C. A 90° pulse of 15 μs was used with a 2 s recycle delay and 512 increments. Three- and four-bond J -coupling effects are observed but no longer-range (5J) couplings are detected. The observed cross-peaks are generally consistent with earlier two-dimensional work [26,29,31]. Points to note are the correlation between the D and E signals, but the lack of a strong correlation between D and any other signal (though there seems to be a weak cross-peak to C). However, we have been able to show that, at least in our solution, the peak to high frequency of that for the main-chain units is composite, with cross-peaks to the signals at both -91.71 and -92.07 ppm. Thus, we extend the assignments of Katoh et al. [29] to the CF_2 group we have labelled A' (Figs. 2 and 3). The spectra therefore show signals for seven CF_2 groups around the reverse-unit position in the chain. There is no off-diagonal correlation between the signals near -107 ppm and any other signal in the spectrum, implying that the relevant fluorines are remote from any other fluorine atoms. This contrasts with the apparent claim by Pianca et al. [31] (implicit in their figure 9, but not actually visible) of correlation with a peak at $\delta_F = -114.3$ ppm, which led these authors to propose end-groups of the type $\text{CH}_3\text{CF}_2\text{CF}_2\text{CH}_2\cdots$ for the peaks near -107 ppm. However, they were dealing with low molar mass PVDF, whereas our samples have high molar mass. Our results suggest the assignment of the -107 ppm peak to branching points, such as $\text{CH}_2\text{CF}_2\text{CH}(\text{CF}_2\text{CH}_2-)\text{CF}_2\text{CH}_2-$, which has been previously deduced [31–33] by use of empirical rules for chemical shifts. Correlations involving other minor peaks are not discussed here.

3.2. Solid-state NMR—assignments of the major signals and discriminating experiments

The direct-polarisation ^{19}F - $\{^1\text{H}\}$ solid-state NMR

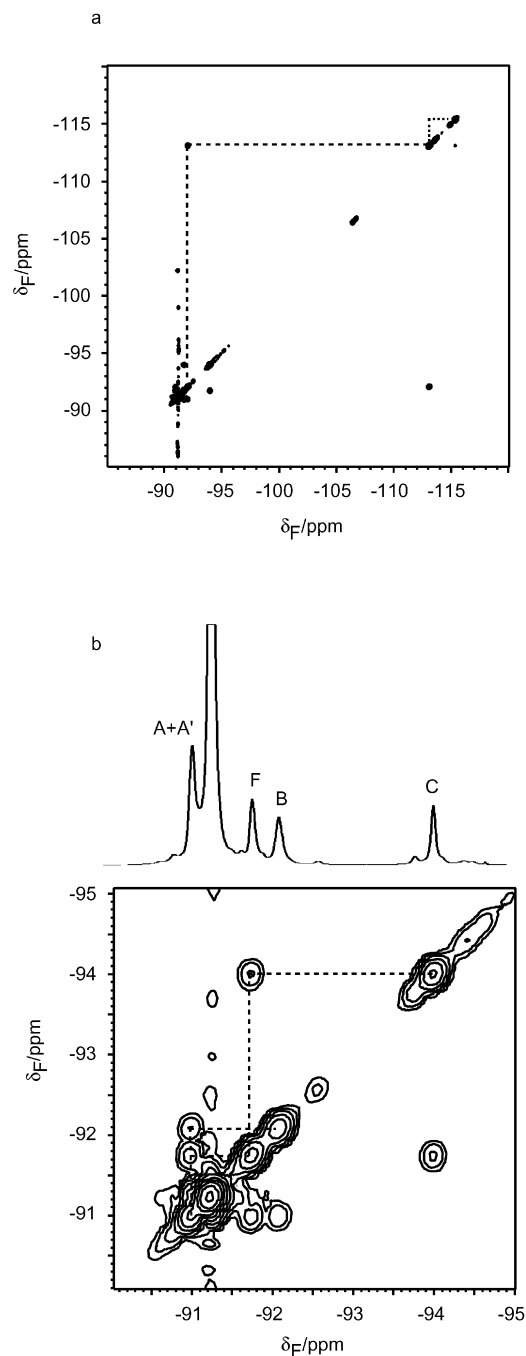


Fig. 3. Proton-coupled 499.78 MHz ^{19}F NMR solution-state COSY spectrum of PVDF in $\text{DMSO-}d_6$ at 22 °C: (a) Full spectrum, showing (B,E) and (E,D) cross-peaks, and (b) expansion of the region -90 to -95 ppm, indicating (A,F), (F,C) and (A',B) cross-peaks. See Fig. 2 for the labelling.

spectrum of Kynar 301F is shown in Fig. 4(a). The chemical shifts and relaxation times are summarised in Tables 1 and 2, respectively. Proton decoupling should remove most, if not all, of the effects from heteronuclear (H,F) coupling [10]. The two nuclei, ^1H and ^{19}F , have comparable abundance and similar values for T_1 : for our sample of PVDF under MAS conditions, $T_1(\text{H}) = 0.51$ s and $T_1(\text{F})$ ranged from 0.57 to 0.63 s for the various fluorine sites, in each case

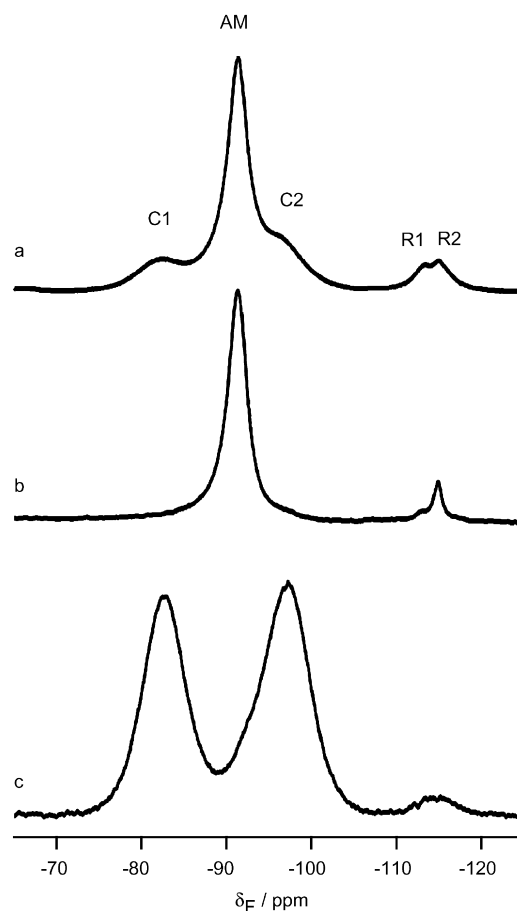


Fig. 4. ^{19}F NMR spectra of PVDF recorded at 60 °C: (a) direct polarisation; (b) direct polarisation with dipolar filter; and (c) direct polarisation followed by a 25 ms ^{19}F spin lock.

measured at 60 °C directly by inversion-recovery (with fluorine decoupling in the former case and with proton decoupling in the latter). Therefore, no significant signal increase would have been gained by adopting a cross-polarisation regime. A comparison of the spectrum with that of the solution state permits the signal AM (-91.2 ppm) to be assigned to the main polymer chain in the amorphous

Table 2

Relaxation measurements of $T_1(\text{F})$ by inversion recovery with proton decoupling, $T_{1\rho}(\text{H})$ by cross-polarisation $\text{H} \rightarrow \text{F}$ with delayed contact time and proton decoupling during acquisition (only), $T_{1\rho}(\text{F})$ by direct-polarisation with varied spin-lock times and H decoupling during acquisition (only), and $T_1(\text{H})$ by inversion recovery with ^{19}F decoupling

	T (°C)	C1	AM	C2	R1	R2
$T_1(\text{F})$ (s)	60	0.63	0.57	N/A	0.59	0.59
$T_{1\rho}(\text{H})$ (ms)	60	14	7.1	13	7.1	6.9
$T_{1\rho}(\text{F})$ (ms)	60	9.5	3.5	N/A	4.1	4.6
	100	6.2	2.9	5.0	3.2	6.2
$T_1(\text{H})$ (s) ^a	60	0.51				

All values result from fitting the experimental data to single-exponential decays and should be considered as average values. N/A = signal not resolved (see Fig. 4(a) for signal assignment).

^a Average over all protons in the sample.

domain. The signals can be further related to sample morphology—see below and also Ref. [10]. The R1 (−113.8 ppm) and R2 (−114.9 ppm) signals are assigned to reverse units, and direct integration of the whole DP spectrum (including spinning sidebands) gives the combined intensity of these signals as 9.3% (Fig. 4(a)), implying a reverse-unit content of 4.7% (compared to a value of 5.5% obtained from solution-state NMR spectra).

Further insight into the origin of the signals, including C1 and C2 (at −82.1 and −95.6 ppm, respectively), with respect to the sample morphology, can be obtained by the use of relaxation filters. Here, the NMR experiment is specifically designed to suppress one component from the spectrum. Two filters have been used in the present study: a dipolar filter [34,35] and a $T_{1\rho}(\text{F})$ filter (Fig. 1(b) and (c)). It should be noted that earlier work [3,10,11] used a $T_{1\rho}(\text{H})$ filter. However, we found that at 60 °C $T_{1\rho}(\text{H})$ values (7.1 and 14.0 ms for the amorphous and crystalline components, respectively, obtained via CP to ^{19}F , with MAS) for our sample have a similar ratio (see below) to the $T_{1\rho}(\text{F})$ values (3.5 and 9.5 ms, obtained by direct polarisation with MAS).

A dipolar filter suppresses signals from strongly dipolar-coupled species. It is, therefore, expected to remove signals originating from relatively rigid material (i.e. crystalline domains). Fig. 4(b) shows the result of such an experiment. The signals C1 and C2 are suppressed and are therefore assigned to the crystalline material of α -PVDF in accordance with the literature [3,8,11]. The remaining intense signal at −92.1 ppm is confirmed as being associated with the amorphous material, in which sufficient molecular motion results in partial averaging of the dipolar coupling. The behaviour of the R1 and R2 signals in this experiment is complex and will be discussed later.

Fast MAS should, in principle, remove the ^{19}F , ^{19}F homonuclear dipolar coupling. However, the spin rate used here does not do that completely, as the dipolar filter would probably then not have any effect.

The measurement of peak heights (following CP from ^1H) under MAS at 60 °C, with a variable-duration spin-lock field equivalent to 80 kHz, shows that the C1/C2 and AM signals for our sample have different $T_{1\rho}(\text{F})$ values: 9.5 ms for C1 and 3.5 ms for AM. Previously published $T_{1\rho}(\text{F})$ values were 20 and 8 ms (at 35 °C) for C1 and AM, respectively [10,11], with a spin-lock field equivalent to 88 kHz. This discrepancy in $T_{1\rho}(\text{F})$ relaxation times probably arises not only because of the differences in the spin-lock fields and temperatures, but also because of variations between the materials such as crystallinity and thermal history [36]. It has been shown that polymer relaxation properties, as monitored by dielectric spectroscopy and dynamic mechanical analysis [37,38], are sensitive to reverse-unit content as well as to the degree of crystallinity.

A $T_{1\rho}(\text{F})$ filter consisting of a 90° pulse followed by a spin-lock pulse of 25 ms duration should give a spectrum favouring signals from that component (C1/C2) of the

sample with the long $T_{1\rho}(\text{F})$, as is seen in Fig. 4(c). It should be noted that this spectrum has a very low absolute intensity (of the order of 5% of the total intensity in the direct-polarisation spectrum) because the spin-lock time is more than twice as long as the longer of the two values of $T_{1\rho}(\text{F})$. Some intensity is retained in the R1/R2 region (see below).

In principle, deconvolution of the direct-polarisation spectrum (Fig. 4(a)) should give information on the relative intensities of the phases present in the material. However, the apparent complexity of the lineshapes and the number of signals potentially present in the spectrum (including sidebands) mean that conclusive data are difficult to obtain. Nevertheless, numerous attempts at deconvolution using Gaussian, Lorentzian and a combination of both lineshapes, suggested that two Lorentzian lines of different widths (760 and 1880 Hz at 60 °C) but at the same chemical shift, best represent the intense AM signal whereas Gaussian lines are appropriate for the C1 and C2 signals. The treatment of the amorphous band as two signals may be an oversimplification, but it is at least mathematically convenient. The amorphous material probably exhibits a range of mobilities and includes some relatively rigid material. Deconvolution of the entire spectrum, including sidebands, suggests that crystalline α -PVDF may account for as little as 30% of the sample, which is in agreement with the value of 28% crystallinity calculated from DSC measurements.

3.3. Variable temperature results

Recently, Su and Tzou [15] investigated the effects of fast MAS at 20, 30 and 35 kHz at ‘ambient temperature’ and concluded that effective suppression of ^1H , ^{19}F dipolar coupling in α -PVDF was reached by a spin rate of 35 kHz. They obtained chemical shift tensor components from spinning sideband intensities, but apparently they did not consider how interplay of the shielding and dipolar tensors may have influenced the detailed distribution of intensities in the spinning sideband manifolds.

Fig. 5 shows the effect on the spectrum of our sample of a variation in controlled temperature at a constant spin rate of 14 kHz (but not on a constant vertical scale). A significant decrease in the AM signal linewidth is seen at elevated temperatures, which causes the C1 and C2 signals to be relatively less prominent. The AM half-height linewidth drops by a factor of ca. 2 from 60 °C (860 Hz, Fig. 5(d)) to 100 °C (430 Hz, Fig. 5(c)). A similar increase in resolution would be seen if an increase in temperature accompanied fast MAS in the experiments of Refs. [13,15]. With no temperature control, the sample temperature at a spin rate of 35 kHz is likely to have been around 65 °C [39]. It is therefore possible that a combination of spin-rate and sample heating was responsible for part of the increased resolution at high spin-rates observed by Su and Tzou. Such effects have recently been reported in detail by Brus [40], who showed that sample heating up to a difference of 58 K could be seen and that MAS-induced heating could affect

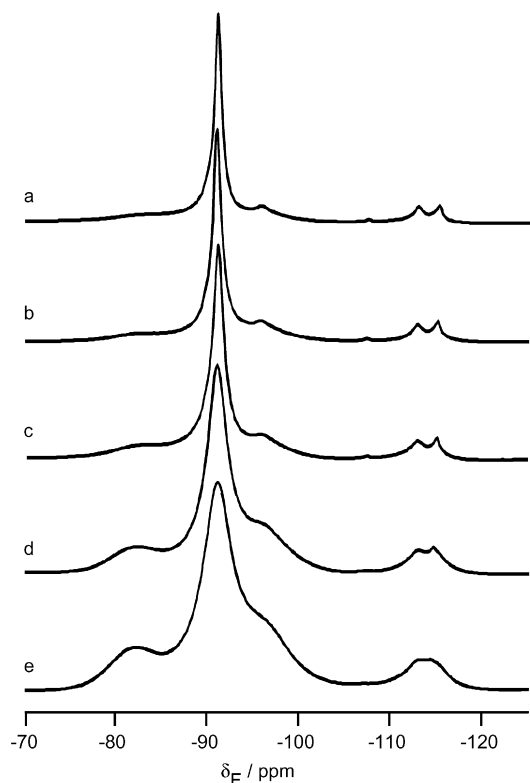


Fig. 5. Direct polarisation ^{19}F NMR spectra of PVDF recorded at (a) 120 °C (b) 110 °C (c) 100 °C (d) 60 °C (e) 20 °C. The spin rate was 14 kHz.

the determination of the isotropic, anisotropy and asymmetry parameters of the shielding tensor. It would seem that temperature control and accurate temperature calibration are required if reliable results are to be produced. The values of $T_{1\rho}(\text{F})$ for peaks C1 and AM at 100 °C (6.2 and 2.9 ms, respectively) are somewhat lower than at 60 °C.

3.4. The minor signals

The signals at -113.8 and -114.9 ppm have been assigned [3,10] to adjacent CF_2 fluorines in the same type of reverse unit as recognised from the solution-state spectrum [22,29], and these have been shown [11] to be associated with the amorphous domains. Our measurements agree, in general, with this conclusion. Thus, at 60 °C, $T_{1\rho}(\text{H})$ values for signals R1 and R2 are 7.1 and 6.9 ms, respectively (compared to 7.1 ms for AM and 14.0 ms for C1). Similarly, $T_{1\rho}(\text{F})$ values are 4.1 and 4.6 ms for R1 and R2, respectively (3.5 ms for AM and 9.5 ms for C1).

However, there is evidence from a number of solid-state experiments (see below), which suggests the situation in this region of the spectrum is more complex. Thus it is apparent from Fig. 4(b) that the reverse-unit signal R1 at -113.8 ppm is suppressed to some extent, along with C1 and C2, by the dipolar filter experiment. This suggests that it may be in some way associated with rigid regions, at least in small part, in contrast to conclusions in the literature [3,10,13] on other PVDF samples. Fig. 4(c) shows that in the

$T_{1\rho}(\text{F})$ -filtered spectrum of the material a broad signal can still be seen in the region corresponding to R1 and R2, again suggesting that there may be some contribution associated with rigid regions. The intensity of the R1 and R2 signals in the $T_{1\rho}(\text{F})$ filtered spectrum (Fig. 4(c)) is 1.4% of the intensity in that region in the unfiltered spectrum. If all of the R1/R2 signal has a $T_{1\rho}(\text{F})$ in common with the amorphous component of the sample (3.5 ms) we would expect only 0.3% of the original signal to be present in the $T_{1\rho}(\text{F})$ filtered spectrum. Thus this residual signal at ca. -114 ppm must have a similar $T_{1\rho}(\text{F})$ to that of the C1/C2 peaks, confirming that it must be closely associated with rigid/crystalline material (i.e. probably at the interface between crystalline and amorphous domains).

However, Fig. 4(b) appears to show an enhancement of signal R2 with respect to the AM peak. There is other evidence for a diversity of behaviour in the R1/R2 region. In order to investigate this anomaly further, we obtained a series of ^{19}F spectra at 100 °C following spin-locking for various times. Even with little or no spin-locking, the anomalous R2 signal is more prominent than at 60 °C, presumably because it is narrower. More remarkably, this peak has a long $T_{1\rho}(\text{F})$ (6.2 ms, compared to values of 6.2, 2.9 and 5.0 ms for C1, AM and C2, respectively, at 100 °C). These data suggest that the anomalous peak is on the extreme narrowing side of a $T_{1\rho}(\text{F})$ minimum. Thus after 25 ms of spin locking the anomalous band has a peak-height similar to that of the AM signal (Fig. 6(a)). In addition, a DPDA experiment with a delay time of 4 ms was used to sample signals with long transverse relaxation times. The spectrum (Fig. 6(b)) is dominated by the -115 ppm signal. Variation of the delay in the DPDA experiment showed

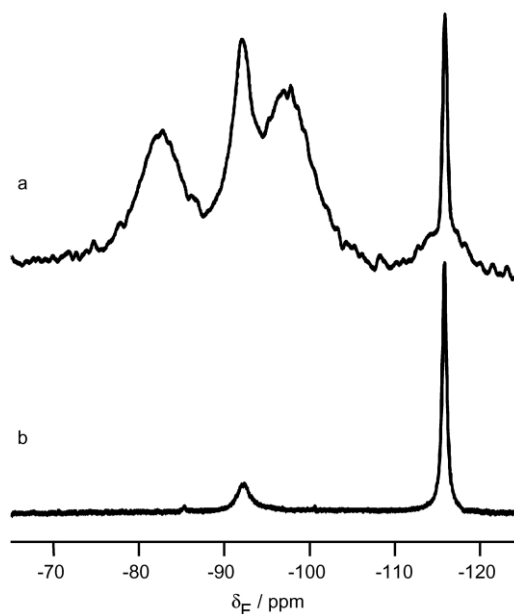


Fig. 6. Direct polarisation ^{19}F NMR spectra of PVDF recorded (a) with a $T_{1\rho}(\text{F})$ relaxation filter with spin diffusion recorded at 100 °C, after 25 ms spin-locking and 1 ms mix time. (b) with a 4 ms delayed acquisition (DPDA experiment) at 60 °C.

approximately exponential decay, with $T_2(\text{F}) \sim 1.2$ ms, for this signal. These experiments suggest that at least part of the R2 signal is associated with very mobile domains, rather than with reversed units in the middle of long chains. Thus there appears to be a region of super-mobility, which could consist of chain ends, short branches, or perhaps occlusions of relatively small molecules of unknown structure. Whereas chain-ends may appear unlikely as an explanation, given that the molecular weight of the polymer (measured at 1×10^6 Da by GPC) implies a maximum of 0.013% for chain-end monomer units, the selectivity of the experiments revealing the relevant signals is very high, and an assignment to $-\text{CF}_2\text{H}$ chain ends seems to us to be the most likely explanation since these have been shown by solution-state NMR to give a signal at $\delta_{\text{F}} = \text{ca.} -114.8$ ppm [28,30,31].

No definitive assignment can be given for the weak signal at ca. -107 ppm (which can be seen in Fig. 5(a)), though we know that it does not have anomalous mobility. It could correspond to end chains of the type CH_3CF_2- , as discussed (see above) for solution-state NMR of VDF oligomers [30,31]. It is more probable that this signal arises from chain-branching. We know from the solution-state NMR spectrum that there is no evidence of branching at CF positions, i.e. no low-frequency signal around -180 ppm, so we suggest that the branching must be at CH centres.

In the solid-state spectrum (Fig. 4) the fluorines of types A, F and B (Fig. 2) would be unresolved from the major signal centred at -91.2 ppm (AM), whilst peak C (Fig. 2) is expected to be obscured by the band at -95.6 ppm (C2).

3.5. Spin diffusion

The addition of a mixing time following selection of the crystalline region by the $T_{1\rho}(\text{F})$ filter experiment (Fig. 1(c), a version of the Goldman–Shen experiment [17]) allows the spin-diffusion from crystalline domain to amorphous domains to be monitored. The signal intensities (peak heights) at 60°C were plotted against the square root of the mixing time (Fig. 7), both for the main amorphous peak (closed circles) and for the reverse-unit signals (open circles). The dimension of the amorphous domains was then

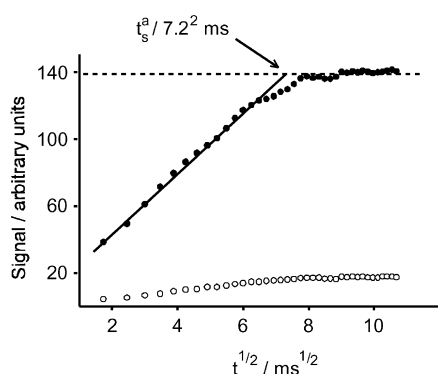


Fig. 7. Peak heights from the spin-diffusion experiment at 60°C for ● the amorphous signal (-91.2 ppm) and ○ signals for the reverse units.

calculated [7,11] using Eqs. (1) and (2)

$$\sqrt{D_{\text{eff}}} = \frac{\sqrt{D_a} \times \sqrt{D_c}}{\sqrt{D_a} + \sqrt{D_c}} \quad (1)$$

$$d_a = \frac{2\varepsilon}{(1 - \chi_c)} \sqrt{D_{\text{eff}} t_s^a / \pi} \quad (2)$$

The effective spin-diffusion coefficient D_{eff} was calculated from the intrinsic spin-diffusion coefficients of the crystalline and amorphous phases, Eq. (1). Here it is assumed that the ratio of spin-diffusion coefficients is determined by the ratio of the static proton linewidths [41]. A ratio of $D_a/D_c = 1 : 6$ has been used [7,11] and the crystalline value $D_c = 0.6 \text{ nm}^2 \text{ ms}^{-1}$, giving the amorphous value as $D_a = 0.1 \times \text{nm}^2 \text{ ms}^{-1}$. The effective spin-diffusion coefficient can then be calculated $D_{\text{eff}} = 0.202 \text{ nm}^2 \text{ ms}^{-1}$ [7].

The characteristic spin-diffusion time t_s^a of 7.2 ms was measured from the plot of diffusion recovery of the amorphous component with the smaller linewidth (Fig. 7) in the usual way [11]. A correction for the effect of T_1 was not made since the phase alternation in the pulse sequence was designed to minimise its effect and the longest mixing time (114 ms) was significantly less than T_1 (0.57 s). A dimensionality factor of $\varepsilon = 1$ [7,11], appropriate to a lamellar morphology, was used. The fractional crystallinity, χ_c was taken to be 30%, as determined from lineshape analysis and in agreement with the DSC measurement of 28%. The amorphous domain size d_a was then determined according to Eq. (2). The value retrieved from this calculation is $d_a = 4.9$ nm, which is in reasonable agreement with the result given by Holstein et al. [11], namely 5 – 7 nm, based on a different set of samples with 50% crystallinity. The similarity of the recovery time of the AM and reverse unit signals is consistent with the conclusion that the reverse units are predominantly incorporated into the amorphous region.

3.6. Recoupling

The dipole–dipole couplings give important information on molecular structure via distance measurements between spins. Weak dipole–dipole couplings yield data on relatively long-range inter-nuclear distances, but these are often obscured by larger contributions to the spin Hamiltonians and they are relatively readily removed by MAS. However, they can be reintroduced into an experiment by either rotor-driven ‘rotational resonance’ or RFDR techniques. For the case where homonuclear recoupling with less sensitivity to the chemical shift than is obtained with rotational resonance is desired, such as correlation spectroscopy of multiple spins over a broad chemical shift range, the coherent averaging of MAS must be disturbed by additional modulation [14,42,43]. In the present work this was achieved by a rotor-synchronised multiple-pulse sequence consisting of a series of π pulses (Fig. 1(a)). The introduction of a $T_{1\rho}(\text{F})$ relaxation filter before the

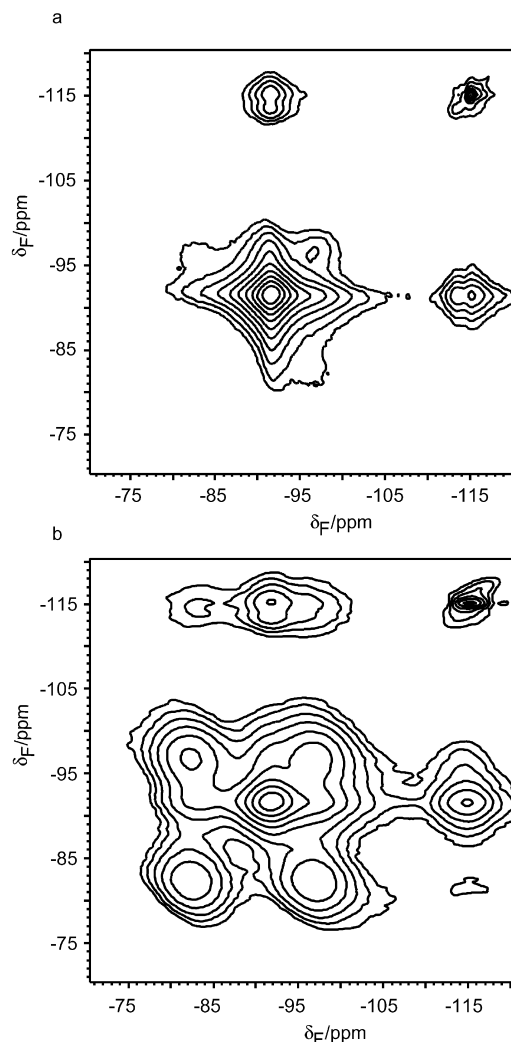


Fig. 8. The 300 MHz ^{19}F NMR RFDR experiment recorded with $n = 7$ at 60 °C (a) without spin-lock filter and (b) with spin-lock filter. Note that for (b) the spin-lock time was 18 ms, shorter than for Fig. 4(c).

recoupling period τ_c (Fig. 1(a)) suppresses much of the dominant signal from the amorphous material and allows a fuller examination of the correlation between coupled species in immobile regions.

The DP-RFDR [14] spectra (Fig. 8) were recorded with and without a $T_{1\rho}(\text{F})$ relaxation filter at a spin rate of 14 kHz and a τ_c (RFDR mixing time) of 4 ms. It can be seen from Fig. 7 that, for short mixing times (of the order of τ_c in the RFDR experiment), spin diffusion from the crystalline to the amorphous domain is limited in extent. The RFDR spectrum (Fig. 8(a)) shows that there are major recoupling interactions between the amorphous region (-91.2 ppm) and the reverse unit signals. The recoupling between the amorphous region (-91.2 ppm) and the reverse unit signal at -113.8 ppm, seen in Fig. 8(a), is no longer so clearly seen in Fig. 8(b) due to the selective nature of the experiment. However, weak cross peaks between crystalline and reverse units are clearly seen from the $T_{1\rho}(\text{F})$ filtered experiment (Fig. 8(b)). This reinforces the conclusion,

reached earlier, that some reverse units are intimately associated with crystalline domains (possibly in interface regions). However, the role of the anomalous signal at -115 ppm in this experiment is not clear.

4. Conclusions

It has been demonstrated that sample temperature greatly influences the spectral linewidth of solid-state ^{19}F NMR high-speed MAS spectra of amorphous-PVDF and that temperature calibration and control is of great importance when evaluating methodologies to achieve line narrowing. We have shown from both dipolar-filtered and $T_{1\rho}(\text{F})$ -filtered experiments that some reverse units, giving a signal at ca. -113.0 ppm, are associated with the rigid domains, though the majority of reverse units are in the amorphous material. The crystalline-selective RFDR spectrum shows recoupling between the crystalline signals and the signal at -115 ppm. The DPDA experiment gives a spectrum of highly mobile material, with part of the R2 signal at -115.0 ppm exhibiting long T_2 relaxation. This observation is consistent with the fact that the R1 signal is apparently suppressed to a greater extent than the R2 signal by the dipolar filter experiment. The presence of such a highly mobile species renders the reverse unit signals more complicated and therefore difficult to decipher. However, we tentatively assign the anomalous signal to $-\text{CF}_2\text{H}$ end-groups. A comparison of our work with that of others shows that $T_{1\rho}(\text{H})$ and $T_{1\rho}(\text{F})$ are probably highly dependent on both reverse-unit content and location as well as the degree of crystallinity.

Acknowledgements

We thank Dr A.M. Kenwright for the solution-state NMR work and for valuable discussions.

References

- [1] Lovinger AJ. *Science* 1983;220:1115.
- [2] Lando JB, Olf HG, Peterlin A. *J Polym Sci* 1966;4:941.
- [3] Holstein P, Scheler U, Harris RK. *Polymer* 1998;39:4937.
- [4] Gregorio R, Cestari M. *J Polym Sci (B)* 1994;32:859.
- [5] Sajkiewicz P, Wasiak A, Gocłowski Z. *Eur Polym J* 1999;35:423.
- [6] Lovinger AJ, Davis DD, Cais RE, Kometani JM. *Polymer* 1987;28:612.
- [7] Schmidt-Rohr K, Spiess HW. *Multidimensional solid-state NMR and polymers*. New York: Academic Press; 1994. Chapter 13.
- [8] Harris RK, Monti G, Holstein P. In: Ando I, Asakura T, editors. *Solid state of NMR polymers*, vol. 84. New York: Elsevier; 1998. Chapter 6.
- [9] Harris RK, Monti GA, Holstein P. In: Ando I, Asakura T, editors. *Solid state of NMR polymers*, vol. 84. New York: Elsevier; 1998. Chapter 18.
- [10] Holstein P, Harris RK, Say BJ. *Solid State Nucl Magn Reson* 1997;8:201.

- [11] Holstein P, Monti GA, Harris RK. *Phys Chem Chem Phys* 1999;1: 3549.
- [12] Ando S, Harris RK, Reinsberg SA. *Magn Reson Chem* 2002;40:97.
- [13] Scheler U. *Bull Magn Reson* 1999;1–4:19.
- [14] Bennet AE, Rienstra CM, Griffiths JM, Zhen W, Landbury PT, Griffin RG. *J Chem Phys* 1998;108:9463.
- [15] Su TW, Tzou DLM. *Polymer* 2000;41:7289.
- [16] Ding S, McDowell AC. *J Phys: Condens Mater* 1999;11:L199.
- [17] Goldman M, Shen L. *Phys Rev* 1966;144:321.
- [18] Vierkötter SA. *J Magn Reson A* 1996;118:84.
- [19] Aliev A, Harris KDM. *Magn Reson Chem* 1994;32:366.
- [20] Teyssedre G, Bernes A, Lacabanne C. *J Polym Sci* 1993;31:2027.
- [21] Nakagawa K, Ishida Y. *J Polym Sci* 1973;11:2153.
- [22] Ferguson RC, Brame Jr. EG. *J Phys Chem* 1979;83:1397.
- [23] Cais RE, Sloane NJA. *Polymer* 1983;24:179.
- [24] Cais RE, Kometani JM. *Macromolecules* 1984;17:1887.
- [25] Ferguson RC, Ovenall DW. *Polym Prepr ACS Polym Chem* 1984;25: 340.
- [26] Cais RE, Kometani JM. *Macromolecules* 1985;18:1354.
- [27] Luttringer G, Meurer B, Weill G. *Polymer* 1990;32:884.
- [28] Russo S, Behari K, Chengji S, Pianca M, Barchiesi E, Moggi G. *Polymer* 1993;34:4777.
- [29] Katoh E, Ogura K, Ando I. *Polym J* 1994;12:1352.
- [30] Herman, Toshiyuki U, Astushi K, Susumu U, Takeshi K, Norimasa O. *Polymer* 1997;38:167.
- [31] Pianca M, Barchiesi E, Esposto G, Radice S. *J Fluorine Chem* 1999; 95:71.
- [32] Yu H, Mi J, Ni H. *Chin J Microwave Radiofreq Spectrosc* 1984;1:372.
- [33] Murascheva YeM, Shashkov AS, Dontsov AA. *Polym Sci USSR* 1981;23:711.
- [34] Schmidt-Rohr K, Clauss J, Spiess HW. *Macromolecules* 1992;25: 3273.
- [35] Egger N, Schmidt-Rohr KL. *J Appl Polym Sci* 1992;44:289.
- [36] McBrierty VJ, Douglass DC. *J Polym Sci, Macromol Rev* 1981;16: 295.
- [37] Shinichi Y. *J Polym Sci* 1970;A2:1057.
- [38] Nabata Y. *Jpn J Appl Phys* 1990;12:2782.
- [39] Bruker Spectrospin. Private communication, mentioned in [Ref. \[15\]](#).
- [40] Brus J. *Solid State Nucl Magn Reson* 2000;16:151.
- [41] Spiegel S, Schmidt-Rohr K, Boeffel C, Spiess HW. *Polymer* 1993;34: 4566.
- [42] Ok JH, Spencer RGS, Bennet AE, Griffin RG. *Chem Phys Lett* 1992; 197:389.
- [43] Bennet AE, Ok JH, Griffin RG, Vega S. *Chem Phys* 1992;96:8624.